Available online at www.sciencedirect.com
SCIENCE DIRECT
Coordination Chemistry Reviews 249 (2005) 2612–2630
COORDINATION CHEMISTRY REVIEWS
www.elsevier.com/locate/ccr

Review

The magnetochemistry of verdazyl radical-based materials

Bryan D. Koivisto, Robin G. Hicks *

Department of Chemistry, University of Victoria, P.O. Box 3065 STN CSC, Vic. BC, Canada V8W 3V6

Received 9 November 2004; accepted 13 March 2005
Available online 18 April 2005

Contents

Abstract

Stable organic radicals have received much attention as building blocks for the construction of molecular magnetic materials because they are readily functionalized using modern synthetic techniques. In this context, the nitroxide radical family has been the dominant class of radicals in molecular magnetochemistry. However, other stable radical systems have also been explored. One such example is the verdazyl family of radicals. Their high chemical stability and synthetic versatility make verdazyls one of the more attractive alternatives to nitroxides in molecular magnet design. This article reviews the magnetism of verdazyl-based systems, including through-bond coupling in polyradicals, coordination complexes and intermolecular interactions in the solid state.

Keywords: Molecule-based magnetism; Stable radicals; Verdazyl radicals

1. Introduction

The pursuit of molecule-based magnetic materials can be described fundamentally as the science of discovering new magnetic building blocks and/or new and improved ways of assembling them. By building block, we mean a spin-bearing entity, for unpaired electrons are a necessary component of all magnetically interesting materials. There are a number of different strategies to assemble spins in molecular-based magnetic materials, including exclusively inorganic-based spins (coordination polymers/metal–organic frameworks), organic

* Corresponding author. Tel.: +1 250 7217 165; fax: +1 250 7217 147.
E-mail address: rhicks@uvic.ca (R.G. Hicks).

0010-8545/$ – see front matter © 2005 Elsevier B.V. All rights reserved.
doi:10.1016/j.ccr.2005.03.012

(radical-containing polymers, molecular crystals of stable radicals) and hybrid approaches in which both metal and radical can be spin active (metal complexes and coordination networks involving radical ligands). The structural and physicochemical diversity in these classes of compounds requires a great deal of fundamental effort to better understand the magnetism of molecular systems en route to new generations of molecule-based magnets.

As noted above, several approaches in molecular magnetism make use of organic radicals as a 'spin-active' component. A basic requirement for a given radical is that it must be stable enough to be prepared, isolated and characterized. This is a severe constraint, as there are few radical classes with sufficient stability to be used for materials science purposes. Significant fundamental advances in intramolecular spin exchange have been realized in systems based on highly reactive radicals [1–5]. However, it is desirable to ultimately develop structure–property relationships in stable radical families. Many otherwise highly reactive or even transient radicals can be rendered kinetically stable through the use of sterically bulky substituents, but the very features providing stability also provide protection from interaction (magnetic or otherwise) with other species. Thus, the most promising spin-active molecular building blocks are those, which do not rely on steric bulk for their stability. Not surprisingly, most efforts in radical approaches to molecular magnetism have focused on nitroxides, arguably the best-known family of stable radicals. Other stable radicals that have received attention as magnetic building blocks include triphenylmethyl-based radicals, phenoxyl-based radicals, heterocyclic thiazyl radicals and radical anions such as those derived from TCNE, TCNQ and quinones.

Verdazyl radicals (tetrahydro-*s*-tetrazin-1-(2H)-yl radicals) have the general structure **1** and are another established class of stable radicals. They do not dimerize in solution or the solid state, and in fact are the only class of radicals that are generally air- and moisture-stable and whose stability does not require bulky substituents. These features make them attractive as potential building blocks for molecular materials. Although verdazyls have not received the same level of attention as the better known nitroxides, there is a body of literature dating back over 30 years concerning the magnetochemistry of verdazyls. Earlier reviews on verdazyls have focused on their synthesis, characterization and chemical properties [6,7]. Herein, we offer a review of the magnetic properties of materials based on verdazyl radicals. General information on the synthesis and characterization of these radicals are provided as a prelude to discussion of systems in which verdazyls may couple magnetically to other spin-systems (verdazyl or otherwise): (a) through bond, (b) through-space and (c) to metal ions in coordination complexes.

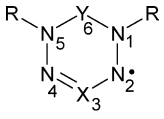

1

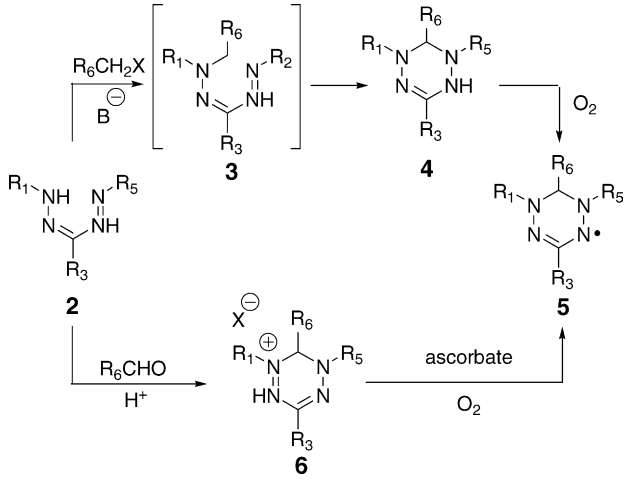

Scheme 1.

2. Verdazyl radical: general considerations

2.1. Syntheses

Verdazyl radicals were discovered by Kuhn and Trischmann in the early 1960s. They reported that attempted alkylation of formazans **2** does not lead to the expected *N*-alkylated formazans; these intermediates, detectable in a few cases, generally rearrange to give tetrazines **4** which are aerobically oxidized to give verdazyl radicals of general structure **5** as grass-green compounds (Scheme 1) [8]. This remains the most common means of making verdazyl radicals with an sp^3 hybridized C6 skeletal atom, and a wide range of verdazyl derivatives have been prepared by this method, including examples of verdazyl-based di-, tri- and polyradicals (vide infra). More recently Katritzky et al. [116] developed an alternative route to verdazyls **5** with a saturated C6 atom. Treatment of formazans with aldehydes in strongly acidic media produces "verdazylium" cations **6** which can be reduced to the neutral radical using ascorbate and air; the ascorbate reduces the ring to an anion (the deprotonated form of **4**), which is subsequently air-oxidized to the radical. These routes lead to verdazyl derivatives with a wide range of alkyl, aryl and other substituents at C3 and C6. However, the N1 and N5 groups are generally constrained to be aromatic due to synthetic limitations in formazan synthesis [9].

The second (and thus far, only other) major synthetic route to verdazyls was reported by Neugebauer and Fischer [10] and Neugebauer et al. [11]. *N*,*N*′-Dialkyl bis-hydrazide reagents **7** (X = O, S) condense with aldehydes to give the saturated tetrazane rings **8**, which can then be oxidized to the corresponding orange-red verdazyls **9** (Scheme 2). A wide range of oxidizing agents have been used, including lead oxide, silver oxide, ferricyanide, periodate and benzoquinone. The verdazyls prepared by this route have a carbonyl or thiocarbonyl group at the C6 position, and it has been demonstrated that the carbonyl group can be reduced to a CH_2 group on the radical, affording *N*,*N*′-dialkyl verdazyls of structure

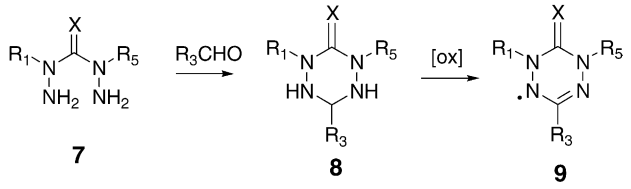

Scheme 2.

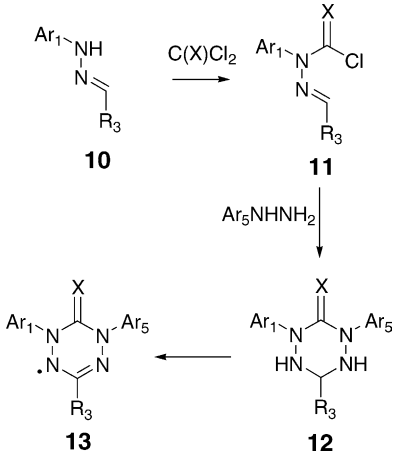

Scheme 3.

5 (where R_6 = H) [12]. This methodology is applicable for a wide range of aldehydes, but limitations in the syntheses of bis-hydrazides **7** require the nitrogen substituents R_1 and R_5 to be methyl or benzyl.

A route to *N*,*N*′-diaryl 6-oxoverdazyls has also been developed (Scheme 3) [13]. Careful reaction of hydrazones **10** with phosgene or thiophosgene yields choloroformyl hydrazones **11** which on treatment with arylhydrazines cyclize to diaryl-substituted tetrazanes **12**. The tetrazanes can then be oxidized to the radical **13** analogously to the *N*,*N*′-dialkyl derivatives described above.

There have been a few reports of inorganic verdazyl analogues in which one of the skeletal carbon atoms have been replaced by phosphorus—so-called "phosphaverdazyl" radicals **14** and **15** [14–18]. The synthetic methodology is conceptually similar to that used for the oxo-/thioxoverdazyls in Scheme 2. No magnetic studies of these compounds have been reported and as such these radicals will not be discussed further.

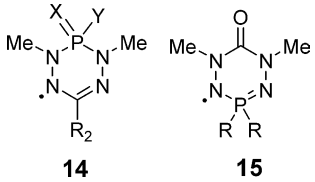

2.2. General properties

A large number of verdazyl radicals have been prepared since their initial discovery 40 years ago. It is convenient

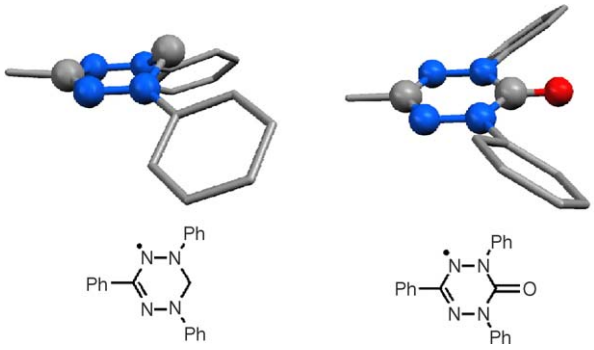

Fig. 1. Conformations of verdazyl rings in 1,3,5-triphenylverdazyl (left) and 1,3,5-triphenyl-6-oxoverdazyl (right). Data from references [19,13], respectively.

to classify these radicals according to the presence or absence of the carbonyl group at C6, as there are subtle but non-negligible differences in the molecular and electronic structures of the two classes. Thus, the two major verdazyl classes **5** and **9** differ essentially by the presence of a saturated (sp3) carbon center in the ring of the former and a carbonyl group in the latter. In the non-carbonyl-containing radicals **5** the saturated carbon lies out of the plane, producing a half-chair conformation as exemplified by the structure of 1,3,5-triphenylverdazyl (Fig. 1) [19]. The so-called "6-oxoverdazyls" **9** are generally fully planar rings, resulting from amide-type resonance involving the carbonyl group and its two flanking nitrogen atoms; Fig. 1 depicts the structure of 1,3,5-triphenyl-6-oxoverdazyl [13]. The three-coordinate nitrogen atoms in both cases remain almost planar—the sum of the angles at these nitrogens in 1,3,5-triphenylverdazyl is 358.7°. The N-aromatic groups are twisted with respect to the plane of the verdazyl, 35° for the oxoverdazyl and between 15° and 25° for the non-carbonyl-containing radicals.

The spin distributions in verdazyl radicals have been established through a combination of experiment and theory. Electron paramagnetic resonance (EPR) spectroscopy played a central – though not the only – role in developing a picture of spin distributions in both classes of radicals. The EPR spectra of verdazyls are generally quite complex, owing to hyperfine interactions with the two pairs of nitrogen atoms and protons on the ring substituents. The situation is further complicated by the near equivalence of the magnitude of hyperfine constants for the two chemically distinct pairs of nitrogen atoms. Consequently, many researchers have resorted to additional techniques in order to gain a full picture of the spin distribution in these radicals. Methods such as electron nuclear double resonance (ENDOR) [20], electron–electron double resonance (ELDOR) [21], dynamic nuclear polarization (DNP) [22] and nuclear magnetic resonance (NMR) [23–27] have all been employed.

The spin distribution in all verdazyls is dominated by the four nitrogen atoms of the heterocycle. Both classes of verdazyls have similar hyperfine coupling (hfc) values for both sets of nitrogen atoms. In the 1,3,5-triarylverdazyls **5**, the hfc's for the two-coordinate nitrogens (N_2 and N_4) and those

of the three-coordinate nitrogens (N_1, N_5) are typically the same within experimental error, ranging from 5.8 to 6G. In comparison, the nitrogen hfc's in the 6-oxoverdazyls **9** differ: the N_2/N_4 values are usually 6.3–6.5G and N_1/N_5 depend on their substituents, having hfc's of ∼4.5–5G when R_1 = aromatic and ∼5.3G when R_1 = alkyl. Hyperfine interactions with protons on the 1,3,5-substituents can also be observed to varying degrees. 1,5-Dialkyl verdazyls have proton hfc's of ∼5.3G, whereas aromatic protons produce values generally under 2G. Substituents on C3 generally give small (<1G) hfc's and are often undetectable by EPR, necessitating the use of ENDOR or NMR for detection.

Calculations on verdazyl radicals range from simple Hückel theory to computationally intense density functional and ab initio post-Hartree–Fock methods, and collectively provide a picture of the electronic structure of verdazyls that is qualitatively consistent with experimental data [28–33]. The $N_1N_2C_3N_4N_5$ fragment of the ring common to both verdazyl types (**5** and **9**) has seven π electrons (the carbonyl group in the oxoverdazyls could also be included, though it is cross-conjugated with respect to the rest of the ring). The odd electron resides in a π* singly occupied molecular orbital (SOMO) **16** spanning the four nitrogen atoms of the ring. The phase properties of this orbital are such that a nodal plane passes through the C3 atom and the bond to substituent R_3. As a result, there is no spin delocalization onto the C3 group and substituent effects on spin distribution are muted. Spin polarization effects do lead to spin density on C3 as well as the substituent, though the extent of spin leakage is generally small. Overall, the four nitrogen atoms carry roughly 80–85% of the total positive spin density and the C3 carbon atom possesses approximately 3–6% negative spin density arising from polarization effects. When the nitrogen substituents R_1 and R_5 are aromatic, spin delocalization and polarization effects lead to spin populations on the aromatic carbons of a few percent. Spin polarization effects alone lead to spin populations on aromatic R_3 carbon atoms of 1% or less. There is also vanishingly small spin on C6 substituents R_6 of non-carbonyl verdazyls **5** because of both the nodal plane in the SOMO and the fact that C6 is not conjugated with the rest of the verdazyl ring.

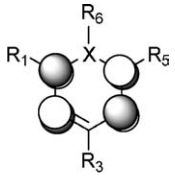

16

3. Magnetic properties of verdazyl radicals

3.1. General considerations

The magnetic properties of molecular systems are in some ways simplified compared to conventional inorganic materials. In purely organic systems, spin–orbit coupling effects are negligible, and it is often possible to accurately make diamagnetic corrections to paramagnetic samples through measurements on diamagnetic analogues of radical compounds. However, understanding magnetism in radical-based materials presents significant challenges. The magnetic properties of crystalline radical samples can be particularly complicated due to a hierarchy of possible magnetic interactions both through-space (intermolecular) and through bond (intramolecular). Understanding these effects usually requires experimental data on both the solid sample as well as for "isolated" molecule to be able to delineate intra- and intermolecular effects and to identify possible exchange pathways based on knowledge of the spin distribution in the radical in question. Even in the absence of through-bond complications, the complex packing patterns, generally weaker exchange interactions that occur through-space and influence on magnetic properties of seemingly minor impurities can render the interpretation of magnetic susceptibility data a serious challenge. For this reason, in order to interpret magnetic data on crystalline solids it is imperative to have crystallographic information on the solid-state structure and molecular packing. Unfortunately such structural data are not always possible, a problem that has surfaced in some of the most important developments in molecule-based magnetism [34] and is an ongoing issue for many molecular systems including verdazyls (see below). With this caveat in mind, the literature covering magnetic properties of verdazyls has been organized into three general classes of exchange interaction: (i) through-bond exchange in verdazyl-based di- and polyradicals, (ii) through-space exchange in verdazyl molecular crystals and (iii) verdazyl-coordination complex magnetochemistry.

3.2. Through-bond magnetism of verdazyl-containing polyradicals: intramolecular coupling

The linking of radicals together through covalent bonds has long been a popular approach to spin coupling in molecular radical systems [35]. Relatively few of these are di- and polyradicals based on verdazyls, although some of the very first magnetic investigations into verdazyl-based materials concerned di- and triradicals. By applying the formazan synthetic methodology to bifunctional precursors, Kuhn et al. prepared a diverse series of verdazyl-based di- and triradicals [36]. Some of these include diradicals **17** and **18** in which verdazyls are connected by *n*-butyl spacers at the ring C3 or C6 atoms, respectively. These were studied by magnetic susceptibility and EPR, echo-modulation spectroscopy [37], NMR and EPR [38], the results of all of which lead to nearly degenerate singlet and triplet states for both molecules. This is not surprising because the saturated butyl linker is electronically insulating, thereby precluding significant intramolecular exchange coupling. It should be noted that no evidence of intermolecular coupling was observed either, though in principle the flexibility of the butyl spacer could permit through-space interactions between the two radical moieties.

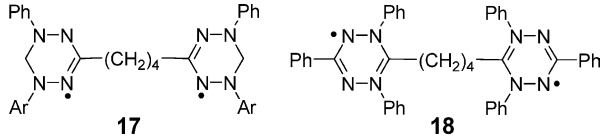

17 18

Other verdazyl containing polyradicals linked by non-conjugated spacers include the tetraradical **19**, comprised of four verdazyls N-linked to a central tetraphenylmethane core [39] and benzene-bridged triradical **20** [40] (the point of attachment—the C3 atom of the radicals to the benzene core is a saturated carbon center, and as such this triradical is considered non-conjugated). In accord with their molecular structures, characterization of possible spin communication in both molecules revealed negligible interactions through a combination of EPR, NMR and magnetic susceptibility studies. The spin-quartet state of **20** was described as "14 cm^{-1} above the doublet ground state", although the spin-state situation is in fact more complex: antiferromagnetic exchange in a three-fold-symmetric triradical such as **20** should lead to spin frustrated behaviour because the three pairwise antiferromagnetic interactions cannot be mutually operative.

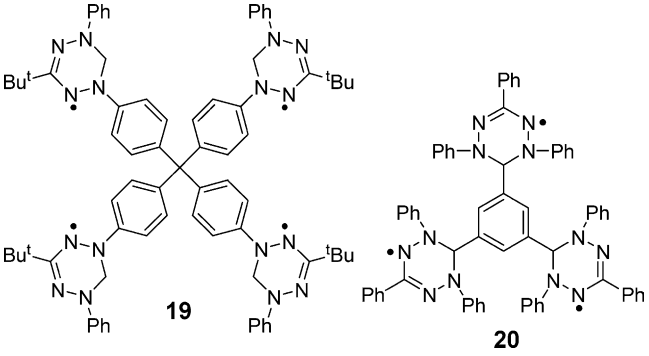

19 20

Broadly related to the non-conjugated di-, tri- and tetraradicals described above are saturated organic polymers containing verdazyls as part of the side chains, e.g. **21** and **22** [41,42]. Weak antiferromagnetic exchange between radical centers is suggested based on the limited physical data, but given the structures of these polymers it seems likely that any measurable interaction would be principally through-space in nature. π-Conjugated polymers incorporating verdazyls are as yet unknown.

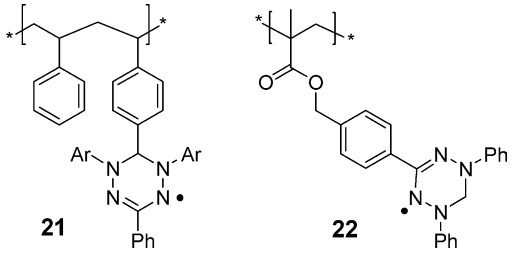

21 22

Intramolecular exchange is generally stronger when the individual spin centers and the molecular substructure which links them are all π-conjugated. Di- and polyradicals of this nature have been well studied theoretically and experimentally, and one of the most important developments has been

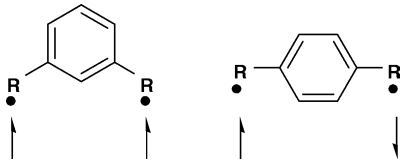

Fig. 2. Topological spin preferences for *m*- and *p*-phenylene bridged diradicals.

a fundamental set of relationships between topological spin distributions and exchange coupling [3,4,35,43,44]. A chief result of this is a general predictability of what sorts of conjugated spacer groups lead to high- or low-spin exchange coupling in conjugated di- and polyradicals. For example, a large number of diradicals are based on odd-electron moieties connected to a central benzene ring. Two radicals linked "meta on a benzene" generally lead to ferromagnetically coupled radicals, while para-linked systems lead to antiferromagnetically coupled systems (Fig. 2). This general rule also requires substantial spin density at the point of attachment to the linker. Thus, in localized diradicals such as *m*-xylylene the triplet state is favoured substantially (>9 kcal/mol), whereas diradicals in which there is little spin density on the adjoining atom are much more weakly coupled and in some cases spin state preferences become subject to other effects, e.g. conformational.

With this in mind, several conjugated verdazyl di- and polyradicals have been constructed by attachment of the verdazyl moiety at either one of the nitrogen atoms or the C3 carbon atom. As discussed earlier, the verdazyl SOMO has a nodal plane that passes through the C3-substituent bond, thereby limiting conjugative spin delocalization. In the Borden and Davidson terminology [43], two SOMOs of the diradical can be confined separately to each radical and as such are disjoint. The small amount of spin density at C6 (through spin polarization effects) would be expected to lead to relatively weak exchange. In contrast, N-linked verdazyl diradicals may be expected to exhibit stronger magnetic coupling because of the substantial spin density on the N atoms. These predictions were in fact made first using simple HMO analyses in 1967 [28].

The first experimentally studied verdazyl polyradicals were the benzene-bridged diradicals **23** and **24**, in which verdazyls are connected via *m*- or *p*-phenylene groups at C3 and the 1,3,5-benzene-centered triradicals **25** (R = H, Me) [36]. Magnetic susceptibility measurements revealed temperature-independent magnetic moments, with values consistent with essentially non-interacting spins (∼2.45 μ_B for each diradical and ∼2.97 μ_B for the triradical). EPR spectra showed some evidence of weak dipolar coupling, although variable temperature spectra were not recorded, thereby precluding determination of the intramolecular exchange. Subsequent studies on the triradical using quantitative, variable-temperature EPR spectroscopy, provided support for the early studies [45]. Kopf et al. carried out paramagnetic NMR studies, the results of which also suggested extremely weak intramolecular ex-

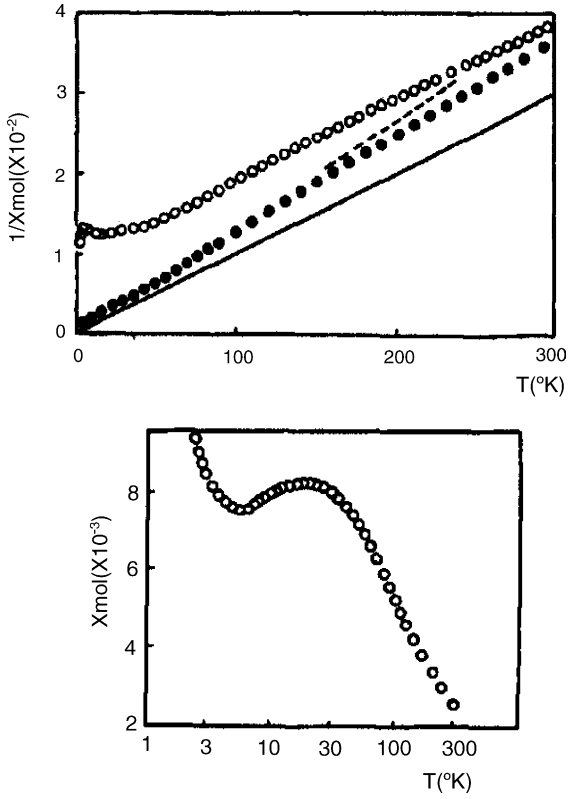

Fig. 3. Top: $1/\chi$ vs. T plots for **23** (open circles) and **24** (filled circles). The solid and broken lines correspond to theoretical Curie–Weiss plots with Curie constants of 1.00 and 0.75, respectively. Bottom: χ vs. T for **23**. Figures taken from [47] with permission.

change in both diradicals [38]. Azuma and co-workers have also examined these diradicals by EPR [46] finding that low-temperature (77 K) spectrum was that of a typical triplet-type species, indicating that a triplet electronic state was at least thermally accessible for both species—although no further EPR information was provided that would allow determination of the ground electronic state.

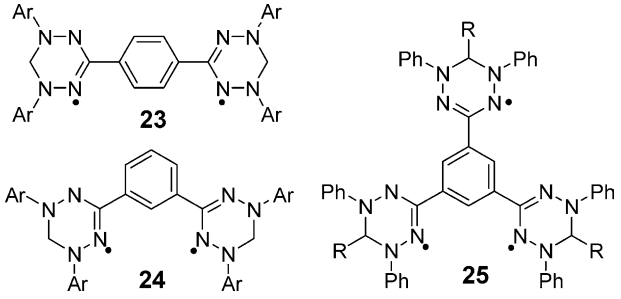

The results described above concerning diradicals **23** and **24** are apparently contradicted by a report claiming that both species possess triplet ground states with exchange energies in excess of 300 K [47]. These conclusions are based on analyses of the $1/\chi$ versus T, magnetic susceptibility data, which the authors claim provides a better fit to $S = 1$ (triplet) rather than two $S = 1/2$ diradicals. However, their plot of $1/\chi$ versus T does not appear to support this conclusion (Fig. 3, top). Moreover, the plot of χ versus T for **23** (Fig. 3, bottom) shows a maximum at 19 K, which suggests weak antiferromagnetic coupling between spins. Interpretation of the solid-state magnetic properties is complicated by the possible presence of both intra- and intermolecular magnetic interactions, and the lack of crystallographic characterization of either diradical precludes any magnetostructural analysis. Nonetheless, the data provided seem to provide circumstantial support of weak antiferromagnetic intramolecular coupling between verdazyls, consistent with the previous studies on these molecules, though further investigations should be undertaken to unequivocally settle this issue.

Benzene-bridged diradical analogues of **23** and **24** based on the "oxoverdazyl" radicals (**26** and **28**) have also been examined, along with a 2,5-thienyl-bridged diradical **27** [48]. The radicals were examined using electrochemical (CV) and spectroscopic (UV–vis, EPR) methods, all of which suggest the radical moieties of each diradical are at best weakly coupled—in each of the diradicals, oxidation of the two radicals (quasi-reversibly or non-reversibly) occurs concurrently, the absorption spectra suggest little electronic overlap of two radicals and Curie plots of the EPR signal intensities are linear which suggest degenerate singlet and triplet states. The instability of these diradicals in the solids state precluded their characterization by magnetic susceptibility measurements.

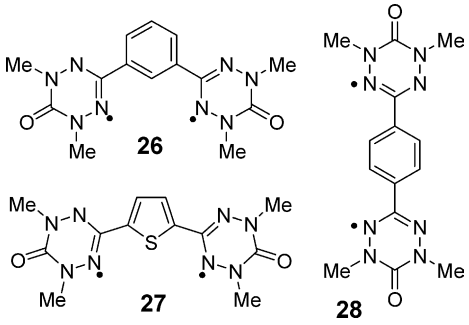

The simplest possible verdazyl diradicals have the two radicals directly attached, i.e. the "spacer" is just a chemical bond between two ring atoms. Several variants of C3–C3′ linked diradicals have in fact been studied. These can be considered to be heteroatom/heterocyclic variants of one of the prototypical disjoint diradicals, namely tetramethyleneethane **32**. The ground spin state preference of the *N,N′,N″,N‴*-tetraphenyl bisverdazyl **29** could not be ascertained due to the instability of this species, although frozen EPR at 88 K do reveal a randomly oriented triplet spectrum [49], suggesting at least a thermally accessible triplet state at this temperature.

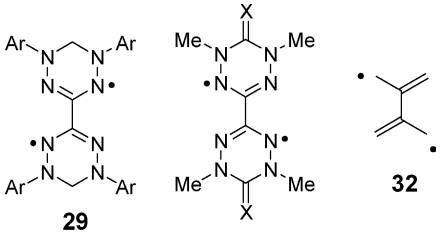

The oxo-based diradical **30** was first reported by Neugebauer and Fischer [10] and its electronic properties were studied thoroughly by Brook et al. [50]. Frozen solutions of the diradical give rise to triplet EPR spectra: the $\Delta m_s = 1$ spectral region was dominated by dipolar coupling and a "half-field" ($\Delta m_s = 2$) transition associated exclusively with the triplet state was observed. A Curie analysis of the $\Delta m_s = 2$ peak afforded a singlet–triplet energy gap of $-760\,cm^{-1}$, i.e. the two radicals are fairly strongly antiferromagnetically coupled. In the solid-state, magnetic susceptibility measurements show effects of both intramolecular exchange coupling as well as intermolecular interactions, in accord with the π stacked structure (see later). Due to the structural complexity, however, quantitative analysis of the magnetic data could not be undertaken in order to determine intra- and intermolecular contributions to the magnetic properties. High-level computational studies (DFT and multiconfigurational SCF methods) on models for diradical **30** and thioxo-analogue **31**, in which the *N*-methyl groups were replaced by hydrogen atoms—are in qualitative agreement: the two verdazyl units are antiferromagnetically coupled, and the calculated strength of the interaction depends on the torsion angle between the two rings. For the planar structure (torsion angle = 0°), calculated exchange energies range from -664 to $-1084\,cm^{-1}$ depending on the computational method [32,51]. As will be discussed in Section 3.4, diradical **30** has been employed as a ligand for transition metals and the coordination of metal ions leads to perturbations of the intramolecular exchange coupling in the diradical.

A final variation on verdazyl-based polyradicals involves linking verdazyls to a spacer via their nitrogen atoms. Given the substantial spin density on these atoms, diradicals linked in this way would be expected to show more substantial intramolecular coupling compared to the previously discussed systems in which verdazyls are connected via their nodal C3 atoms. This has proven to be so for a series of such diradicals **32** [36,52,53]. The simple *p*-phenylene bridged diradical **32a** appears to be fully diamagnetic even at room temperature, and as the number of *p*-phenylene linkages increases there is a gradual evolution to true biradical behaviour; diradicals **32b** and **32c** have exchange energies of -210 and $-35\,cm^{-1}$ based on dimer model fits to magnetic susceptibility data, and **32d** is essentially a true biradical. Isomeric biphenylene diradicals **32e** and **32f** are comparable to **32b** in terms of exchange energy, while the naphthalene-bridged systems **32g** and **32h** are somewhat more strongly coupled ($J \sim -525\,cm^{-1}$). These numbers should be interpreted with caution because the magnetic data were obtained on solid samples—thereby raising the possibility that intermolecular interactions might be contributing to the magnetic properties. However, the proposed closed-shell doubly zwitterionic resonance contributors (shown as **32a′** for derivative **32a**) which would account for the strong intramolecular antiferromagnetic electronic coupling is corroborated by their solution UV–vis–NIR spectra: the most strongly coupled diradicals – **32a**, **b**, **g**, **h** – have significantly red-shifted and temperature dependent UV–vis spectra, whereas the spectra of the most weakly coupled ones – **32c**, **d** – resemble those of the parent triphenylverdazyl radical.

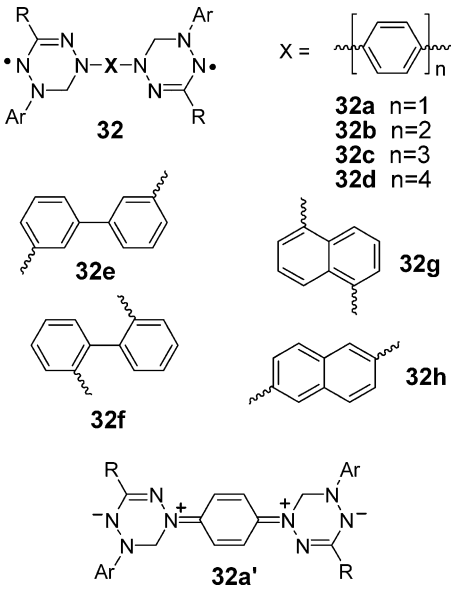

There are very few example of "heterospin" verdazyl systems involving through-bond coupling between a verdazyl and a different radical moiety. Lahti and co-workers prepared an azide-substituted verdazyl **33** and used it to generate a verdazyl-nitrene hybrid **34**, which was characterized in situ using EPR and electronic spectroscopy. The $S = 3/2$ spin state so characterized was found to be similar in nature to other polyradicals in which a nitrene is para to a second radical center [54].

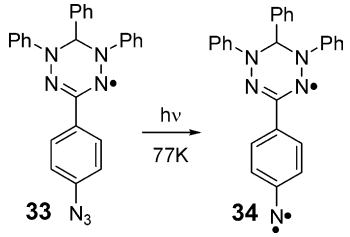

The only other verdazyl-based heterospin systems of note represent a somewhat different concept towards magnetic coupling, namely the observation of intermolecular exchange in photoinduced excited states [55–57]. The ground states of compounds **35** and **37** only possess verdazyl-based spins, and consequently have EPR spectra typical of 1,5-dimethyl-6-oxoverdazyl derivatives; similarly, Curie analysis of diradical **36** in its ground state suggests very weak antiferromagnetic exchange ($\sim -2\,cm^{-1}$). However, upon continuous irradiation, time resolved EPR spectroscopy (TREPR) permits observation of signals readily assigned to spin quartet ($S = 3/2$) species in the case of **35** or **37**, and a spin quintet ($S = 2$) spectrum for **36.** These arise from photoexcitation of the anthracene or pyrene moieties to produce excited state triplets, which can then interact ferromagnetically with the $S = 1/2$ verdazyl radical substituents. Density functional calculations

on the excited states provide spin distribution maps that are consistent with this spectral interpretation. These molecules can therefore be considered as prototypes for organic photomagnetic materials [58].

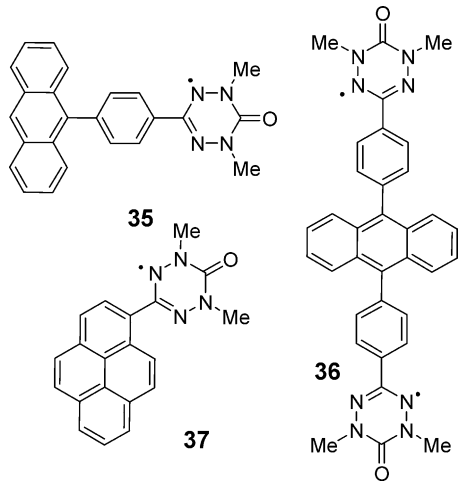

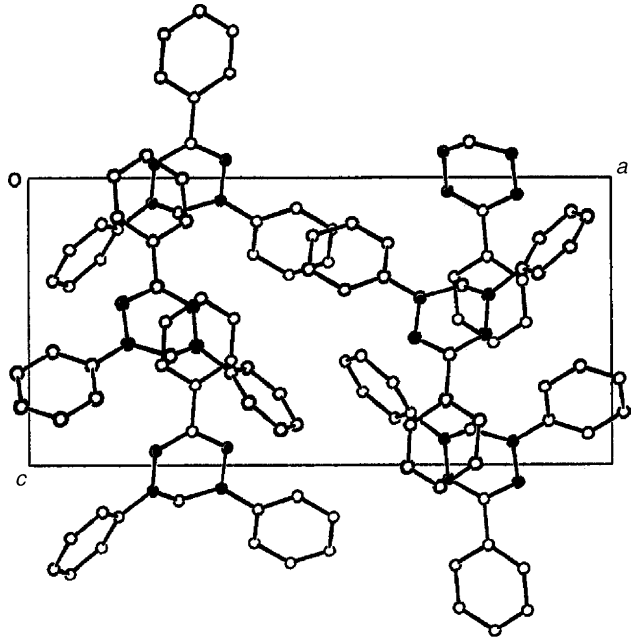

Fig. 4. Packing diagram for 1,3,5-triphenylverdazyl. Reproduced from [19] with permission. Nitrogen atoms are black.

3.3. Through-space magnetic interaction in verdazyl radical molecular crystals

3.3.1. General

Investigations of the magnetic properties of radical-based molecular crystals are extensive within the molecular magnetism community. The challenges in this area are considerable, as the combination of relatively weak magnetic interactions through-space (compared to intramolecular) coupled with the complex packing patterns adopted in molecular materials can render the development of structure–property relationships very difficult. Even in very well studied materials such as nitroxide radicals, where there is ample magnetic and structural data, a basic understanding of how intermolecular magnetic interactions are dictated by distance and relative orientation of spin centers is still lacking [59,60]. It is therefore worthwhile to examine different radical systems in the hopes of uncovering such structure–magnetism correlations. Verdazyl radicals, with their near-planar or planar structure and general stability even in the absence of bulky substituents, are an attractive alternative to nitroxides as building blocks for through-space interactions. Indeed, there have been many reports of magnetic phenomena in verdazyl-based crystals stemming back to 1970. Unfortunately many of these studies report magnetic data and do not include crystal structures of the materials in question. In molecular crystals, more than any other general class of material, structural information is vital to being able to interpret magnetism in a meaningful way. For this reason this review will focus more on the systems for which structural details are available to aid in interpretation of magnetic characterization, though all relevant magnetic data for other verdazyl-based systems will at least be mentioned.

3.3.2. Structurally characterized examples

One of the very first verdazyl radicals (and indeed any stable radical) to be magnetically and structurally characterized is 1,3,5-triphenylverdazyl. A packing diagram for this molecule is shown in Fig. 4 [19]. The radicals lie in the ac plane and adopt a layered structure in which the C3 phenyl substituents are partially superimposed over/under the central verdazyl ring of adjacent molecules along the *b*-axis. The *N*-phenyl groups interleave with one another parallel to both the *a* and *c* directions. The closest intermolecular contacts in this structures are some C–N contacts between 3.8 and 4.0 Å, i.e. beyond the van der Waals contact distance for these atoms. There is no N–N contacts within 4 Å.

The magnetic properties of 1,3,5-triphenylverdazyl were first reported in 1973 [61]. The susceptibility follows Curie–Weiss behaviour ($\theta = -8$ K) but deviates from this at lower temperatures, as the susceptibility χ reaches a maximum value at 6.9 K and then drops off. This behaviour is qualitatively consistent with a Heisenberg-type linear magnetic chain model exhibiting antiferromagnetic interactions. However, below T_{max} the drop-off in susceptibility does not fit this model and the susceptibility abruptly increases at 1.7 K. Heat capacity studies confirm the transition to a magnetically ordered state at 1.7 K [62]. Tomoyishi et al. also found a magnetic transition at 1.78 K, which they ascribed to weak ferromagnetism associated with antiferromagnetic ordering [63]. Thus, although the ordering is antiferromagnetic, the susceptibility increases below T_N because the one-dimensional magnetic chains adopt a spin-canted magnetic structure. Interestingly, neutron diffraction studies revealed that, as predicted

by Azuma et al. [61], the antiferromagnetic chain direction is most likely parallel to the *c*-axis.

The magnetism of 1,3,5-triphenylverdazyl serves as a useful point of departure from which to discuss the magnetism of other verdazyl-based molecular crystals. Some of the qualitative structural and magnetic features of this radical are common to many other verdazyls. From a structural perspective, several other verdazyl derivatives which have been crystallographically characterized adopt crudely similar structures, i.e. layered-type structures with non-superimposed stacking motifs not unlike that of 1,3,5-triphenylverdazyl in which aromatic substituents are pseudo-aligned with verdazyl rings. However, as has been found to be the case with nitroxide type radicals [59,60], attempts to correlate structural particulars with observed magnetic properties in verdazyls turns out to be less than straightforward. The 1,3,5-triarylverdazyl derivatives **38–40** share broadly similar solid-state structural traits – layered structures, poor/incomplete π stacking involving the verdazyl ring and aromatic substituents – and none have significant intermolecular contacts below 3.5 Å. Yet, the di-*p*-tolyl compound **38** [64,65] and *p*-chlorophenyl derivative **40** [66] both exhibit relatively strong intermolecular antiferromagnetic interactions. Similarly to triphenyl verdazyl, **38** and **40** deviate from Curie–Weiss behaviour ($\theta = -14.6$ K for **38** and -18 K for **40**) in a manner modelled as one-dimensional Heisenberg chains ($J = -10\ \mathrm{cm}^{-1}$ for **38** and $-11.4\ \mathrm{cm}^{-1}$ for **40**). In contrast, the susceptibility versus temperature profile for **39** shows Curie–Weiss behaviour down to 1.8 K with a Weiss constant of -1 K, suggesting only very weak general antiferromagnetic coupling in this radical [67].

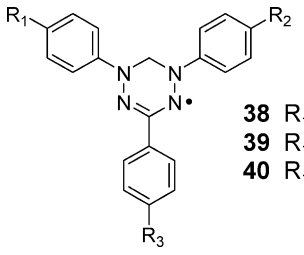

38 R_1 = H, R_2=R_3=Me
39 R_1=R_2=R_3=Me
40 R_1=R_2=H, R_3=Cl

Other verdazyl derivatives with stacking motifs at first glance would seem to be more amenable to magnetostructural analysis, but again the complexities of intermolecular interactions in radical molecular crystals prove to be challenging to understand on a microscopic/molecular level. The three nitro-containing verdazyls **41–43** illustrate this point. All three compounds adopt slipped one-dimensional stacks in the solid state. 3-Nitro-1,5-diphenylverdazyl **41** possesses stacks that are moderately offset along the molecular long axis such that there is still partial overlap of the verdazyl rings within the π stacks (Fig. 5a) [68]. The interplanar separation of ∼3.5 Å is just beyond the van der Waals separation for aromatic π systems and is likely due to the twisting of the *N*-phenyl rings which forces the radicals further apart. This material exhibits one-dimensional Heisenberg chain-like behaviour ($J = -4\ \mathrm{cm}^{-1}$). The 3-(*p*-nitrophenyl) analogue **42** possesses one-dimensional stacks similar to those seen in **41**, with a similar extent of longitudinal shifting. The magnetic data also appear to support intermolecular antiferromagnetic interactions (the magnetic moment decreases at low temperatures), though no modelling of the magnetic susceptibility was reported. The introduction of a phenyl substituent to the saturated (C6) ring carbon in **43** leads to a significant solid-state change: although one-dimensional stacks are retained, the steric requirements of the 6-phenyl substituent – which protrudes upwards nearly perpendicular to the plane of the verdazyl ring – causes severe slipping of the molecules within the π stack, such that verdazyl rings are now partially superimposed over the 3-nitrophenyl group, which has very little spin density associated with it (Fig. 5b). The magnetic susceptibility of this radical reveals intermolecular ferromagnetic interactions—the first time ferromagnetic behaviour had been seen in a verdazyl-based material [69]. Analysis of the temperature dependence of the magnetic susceptibility using a quasi-one-dimensional Heisenberg ferromagnetic chain produced an intrachain interaction $J = +2.5\ \mathrm{cm}^{-1}$. At 1.1 K, this compound undergoes a change to an antiferromagnetically ordered state, providing another example of a verdazyl-based solid that magnetically orders. Wudl et al. rationalized the ferromagnetic interactions by invoking the "McConnell I" mechanism [70] in which intermolecular ferromagnetic interactions are favoured when atoms possessing positive spin density interact with atoms possessing negative spin density on neighbouring molecules. The verdazyl nitrogen atoms carry the bulk of positive spin density, while the *p*-nitrophenyl group should be spin polarized to yield spin density alternating in sign on adjacent ring atoms. Given the fairly weak nature of the ferromagnetic coupling and the non-ideal superposition of the verdazyl and phenyl rings it is not clear whether this mechanism is operative (nor can magnetic interactions involving the *N*-phenyl groups, which are also spin polarized to a lager extent than the C3 substituent, be ruled out).

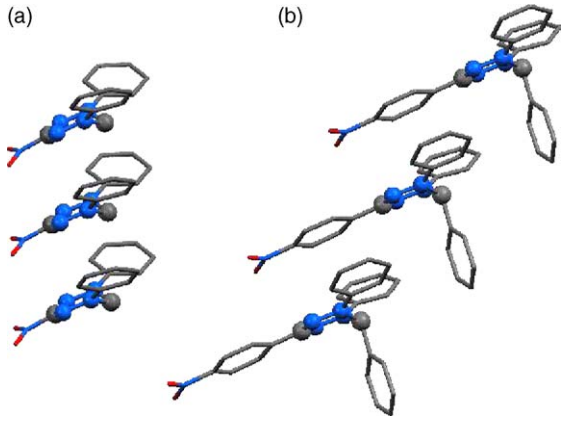

Fig. 5. One-dimensional stacking of verdazyls: (a) **41** and (b) **43**. Data taken from [68].

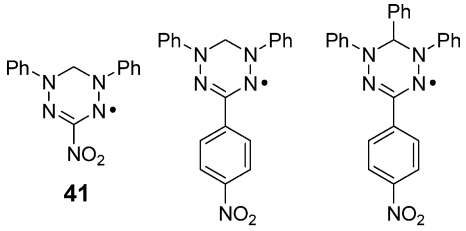

The stacked structure of **43** is unusual in that other verdazyl derivatives with Me of Ph substituents at C6 generally do not adopt stacked structures because of the steric requirements of the C6 substituent. Compounds **44–47** are examples of such structures. The absence of molecular stacks does not correlate well with the absence of intermolecular magnetic interactions. The magnetism of 6-methyl-3-nitro-1,5-diphenylverdazyl **44**, for example, can be modelled above 100 K with a relatively large Weiss constant of −18 K (the magnetic properties in the low-temperature region deviates from Curie–Weiss behaviour in a manner that is not well understood) [68]. In contrast, 6-methyl-1,3,5-triphenylverdazyl **45** was in fact modelled using a Heisenberg chain ($J = -7\,cm^{-1}$) despite the apparent absence of an obvious physical pathway to explain the model [71]. 1,3,5,6-Tetraphenylverdazyl **46** exhibits strong interactions ($\theta = -22$ K), whereas the 1,3,5,6,6-pentaphenyl analogue is nearly a Curie paramagnet ($\theta = -0.1$ K) [72]. The latter may be rationalized on the basis that the five phenyl groups serve to effectively insulate verdazyl spins from one another in the solid state. Regarding the other compounds, however, the relationships between molecular packing and observed magnetism are far from understood. Given the relatively inefficient packing in all of these derivatives discussed so far, the magnetic interactions tend to be very weak and therefore a function of packing patterns and spin distributions [73] on a much more subtle level than otherwise expected.

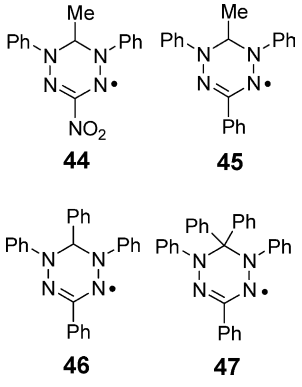

There is but one example of a verdazyl radical exhibiting truly eclipsed stacking of the central verdazyl moieties, namely 3-(4-fluorophenyl)-1,5-diphenylverdazyl **48** (Fig. 6) [74]. The intrastack N–N contacts are roughly 4 Å apart, which on its own would suggest that intermolecular magnetic interactions should be relatively weak. However, the magnetic susceptibility of this radical is quite unusual. A broad maximum in χ versus T is seen at 200 K—approximately one order of magnitude higher in temperature than typically seen in verdazyl radical crystals. As seen in Fig. 7, these data cannot be fit to standard Heisenberg one-dimensional chain or dimer models, but qualitatively the strength of the magnetic interactions must be on the order of $-200\,cm^{-1}$ to account for the susceptibility data. Deviations from one-dimensional behaviour were proposed based on the substantial spin density predicted on the *N*-phenyl groups, leading to quasi-two-dimensional type behaviour (no analytical expressions for the magnetism of these systems were available). Qualitatively similar magnetic behaviour – very strong antiferromagnetic interactions, data that cannot be fit to standard low-dimensional models – was found in two other verdazyl radicals **49** and **50**, although no crystallographic data were available with which to attempt to correlate the magnetic properties. Nonetheless, these compounds demonstrate the potential for very large through-space exchange interactions in radical-based molecular crystals.

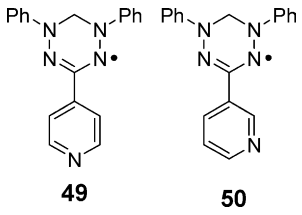

Another verdazyl that appears to exhibit very strong intermolecular antiferromagnetic exchange is the 3,3′-bis(6-oxoverdazyl) diradical **30** [50]. This diradical adopts a herringbone-type packing pattern in the solid state (Fig. 8). Nearest neighbour diradicals within the slipped stacks are offset both longitudinally and laterally (Fig. 8, inset) but the smaller *N*-methyl substituents and truly planar nature of the 6-oxoverdazyls permit more efficient packing: the interplanar separation is only about 3.2 Å. The χT versus T plot for this substance drops off rapidly with temperature but in a manner that could not be modelled. The complex bulk magnetic behaviour undoubtedly arises from the fact that there is strong intramolecular exchange coupling within each diradical in addition to through-space effects. Based on the qualitative temperature dependence of the magnetic susceptibility, it is probable that the intermolecular exchange is on the order of $-100\,cm^{-1}$.

Only two other single component neutral 6-oxoverdazyl radicals have been structurally and magnetically characterized, and both derivatives adopt qualitatively similar structures. Both 1,3,5-triphenyl-6-oxoverdazyl **51** [13] and 1,5-dimethyl-3-(2-pyridyl)-6-oxoverdazyl **52** [75] adopt antiparallel one-dimensional stacked structures in which the aromatic 3-substituent is well superimposed over/under neighbouring verdazyl rings within the stack (depicted schemati-

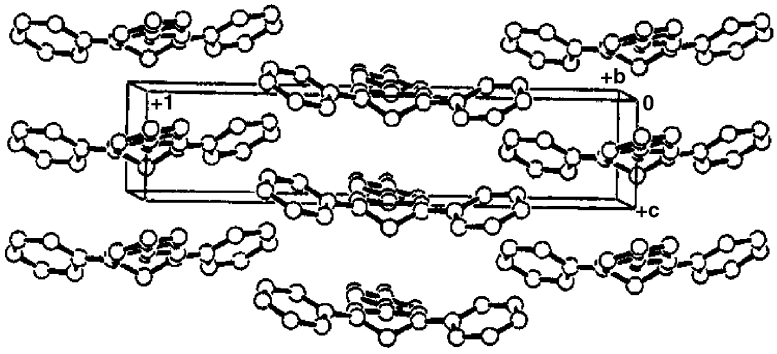

Fig. 6. Packing diagram for **48**. Reproduced from [74] with permission.

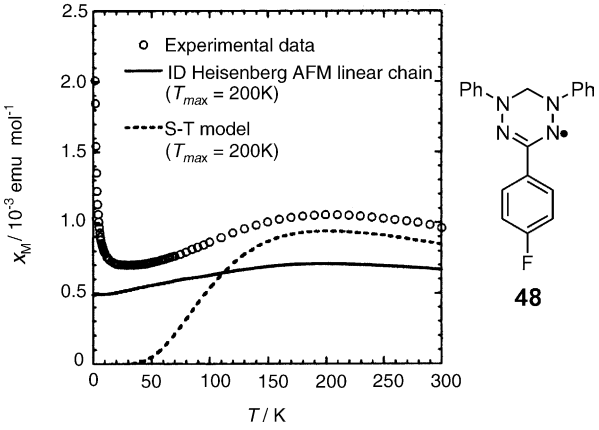

Fig. 7. Molecular structure and χ vs. T plot for **48**. Reproduced from [74] with permission.

cally in **53**). The *N*-phenyl substituents in **51** are significantly twisted with respect to the verdazyl plane, which may explain the rather large interplanar separation of 3.65 Å within the molecular stacks. In comparison, the *N*-methyl groups of **52** offer no such impediment and the interplanar spacing in this structure is ~3.4 Å.

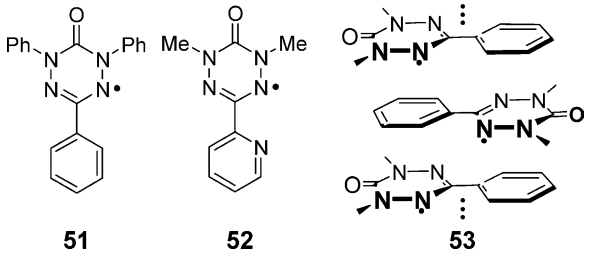

To a first approximation, the magnetic properties of **51** and **52** reflect their relative intrastack packing efficiency. Thus, the temperature dependence of the magnetic susceptibility of both substances can be fit using a one-dimensional Heisenberg linear chain model. For **51**, the intrachain exchange energy is fairly weak ($J = -5\,cm^{-1}$) [76], whereas for **52** the calculated value is about an order of magnitude stronger ($J = -56\,cm^{-1}$) [75], suggesting that intermolecular exchange interaction energies are very sensitive to intermolecular distances at or around the van der Waals limit.

Further details of the magnetochemistry of both **51** and **52** warrant comment. As mentioned, the magnetic properties of **51** can be modelled as a Heisenberg antiferromagnetic chain—but only down to the temperature at which the susceptibility reaches a maximum. Below this temperature, the decrease in χ is only slight and does not follow the Heisenberg model. Below 5 K the susceptibility sharply rises, signalling the onset of bulk magnetic order. The ordering is antiferromagnetic but canted, giving rise to weak ferromagnetism below 5 K. This is one of the highest magnetic ordering temperatures seen in purely organic substances.

Radical **52** does not magnetically order but does present a conundrum in terms of the current paradigms for rationalizing strong intermolecular exchange interactions. Strong through-space magnetic exchange interactions are normally correlated with close intermolecular contacts between atoms that bear a large spin density. However, in the crystal structure of **52** the closest contacts between such atoms – the four verdazyl nitrogen atoms – are over 4 Å apart, too far to explain the observed strong exchange interactions. Moreover, there is too little spin density on the pyridyl ring for a Mc-

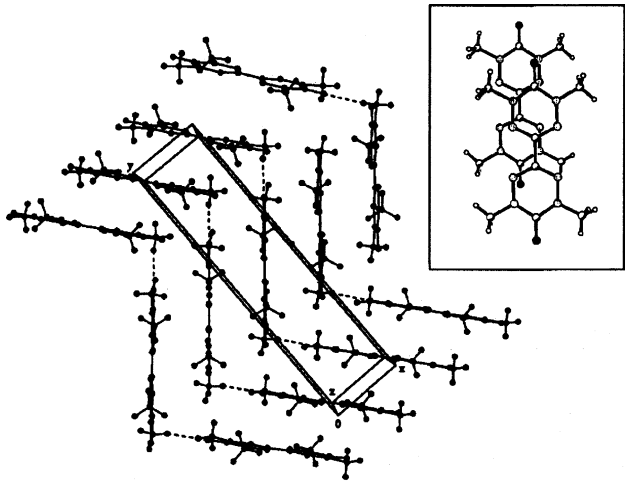

Fig. 8. Packing diagram for diradical **30**. Inset shows superposition of neighbouring molecules within a stack. Reproduced from [50] with permission.

Connell 1 type mechanism to produce an exchange interaction of this magnitude. Therefore, spin density arguments alone fail to account for the strong exchange. A "supramolecular superexchange" pathway was proposed in which a π* orbital on pyridine with appropriate symmetry mediates exchange between radicals (cf. **54**). DFT calculations on model stack triads provided support for this mechanism, which has significant implications for the ways in which the magnetism of molecular crystals are considered: the radicals within the stacks of **52** are nearly 7 Å apart yet are still able to magnetically communicate fairly strongly.

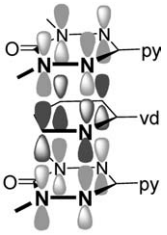

54

3.3.3. Magnetism of verdazyls not structurally characterized

The solid-state magnetic properties of a large number of verdazyl radicals have been reported for which no crystallographic characterization is available. Because these compounds have not been characterized crystallographically, it is not possible to explain the origins of their magnetic behaviour. A summary of the magnetic properties of these compounds are presented in Table 1. Notable general features are the propensity of one-dimensional chain models, which may hint at π stacked structures of some sort—not an unreasonable supposition given the preponderance of various stacked structures in crystallographically characterized verdazyls. A variety of low-temperature phenomena has been observed, including ferromagnetic ordering, weak (canted) ferromagnetism, spin-Peierls transition and alloying effects of solid samples of two different radicals [77–80]. Again, however, no manner of analysis of the bulk magnetic properties on the basis of variation in molecular structure can be considered anything other than circumstantial in the absence of crystallographic data, specifically details of the packing of molecules in the solid state.

3.3.4. Verdazyl-based radical ion salts

Systems in which the verdazyl radicals are part of a cationic component of a salt are treated separately in part because the anions involved are also potentially active magnetic or conducting components. The general strategy here has been to prepare verdazyl radicals with cationic substituents and combine them with radical anions such as $TCNQ^-$ or $M(dmit)_2^-$, both of which have been extensively employed in conducting molecular materials, in the hopes of generating multifunctional materials with cooperative charge transport and magnetic properties. Thus, a series of 3-(*N*-alkyl pyridinium)-verdazyl salts of TCNQ have been reported [91,92]. Alkylation of the 3-(4-pyridyl)- and 3-(3-pyridyl)-1,5-diphenylverdazyls with alkyl iodides afforded the *N*-alkylpyridinium iodide salts. Metathesis reactions with LiTCNQ gave the 1:1 TCNQ complexes of the verdazyl-based cations, and reaction of these salts with one equivalent of neutral TCNQ produced the corresponding 1:2 salts (Scheme 4). The charge transport and magnetic properties of all eight TCNQ salts were reported, but the only structurally characterized compound is the 1:2 complex of the *N*-ethyl-4-pyridinium radical cation [**55**$Et^+(TCNQ)_2^-$]. The physical properties of the eight salts are summarized in Table 2.

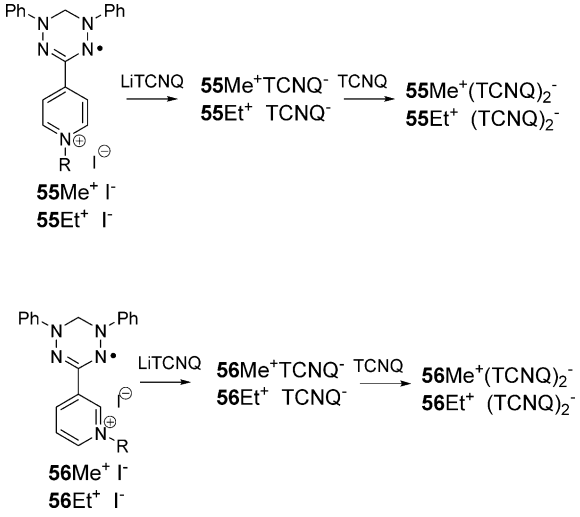

Scheme 4.

The 1:1 salts are all insulators in accord with either isolated TCNQ radical anions or dimers thereof. The 1:2 salts are semiconductors, consistent with non-integral oxidation state of anion. Magnetically, the 1:1 salts show weak antiferromagnetic interactions that generally were not modelled. The room temperature moments of the 1:1 salts are most consistent with π-dimerized (diamagnetic) TCNQ anions and free, isolated $S = 1/2$ verdazyl spins which then couple weakly and antiferromagnetically at low temperatures.

The magnetic susceptibility of **56**$Et^+(TCNQ)_2$ has a plateau in the χT versus T plot between 200 and 50 K, at a value corresponding to isolated $S = 1/2$ spins, most likely the verdazyl cation radical—the TCNQ spins are paired. At lower temperature, weak antiferromagnetic interactions between the verdazyls are seen. Above 200 K, the moment increases, indicative of thermal excitation of TCNQ to excited triplet states. The high-temperature region can be fit using a dimer model with $J_{dimer} = -257\ cm^{-1}$. This model can be understood based on the crystal structure of this salt (Fig. 9), which consists of pseudo-isolated verdazyl radical (cations) and tetrameric stacks of TCNQ molecules (i.e. two dimers). Similar models were employed to fit the magnetic data for

Table 1
Magnetic characterization of verdazyl lacking in crystal structure

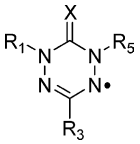

X	R_1	R_5	R_3	Magnetic properties[a]	References
H_2	Ph	*p*-$MeOC_6H_4$	Ph	Linear ising, $J \sim 11.8\,cm^{-1}$ (footnote poor fit)	[81]
H_2	Ph	*p*-BrC_6H_4	Ph	CW, $\theta = -1.8$ K	[72]
H_2	Ph	*p*-$^{i}PrC_6H_4$	Ph	CW, $\theta = -1.3$ K	[72]
H, 1-naphthyl	Ph	Ph	Ph	CW, $\theta = -0.5$ K	[72]
H, 2-naphthyl	Ph	Ph	Ph	CW, $\theta = -0.5$ K	[72]
H, *p*-BrC_6H_4	Ph	Ph	Ph	CW, $\theta = -0.6$ K	[72]
S	Me	Me	*p*-ClC_6H_4	CW, $\theta = +3.2$ K; ferromagnetic order; $T_C = 0.7$ K	[82–85]
S	Me	Me	*p*-BrC_6H_4	Heis. Reg., $J = -14\,cm^{-1}$	[82–85]
O	Ph	Ph	*p*-ClC_6H_4	CW; $\theta = +2.5$ K	[86]
O	Ph	Ph	*p*-BrC_6H_4	CW; $\theta = -7.7$ K	[86]
S	Ph	Ph	Ph	Heis. Alt.; $J_1 = -23\,cm^{-1}$, $J_2 = -14\,cm^{-1}$	[86]
S	Ph	Ph	*p*-ClC_6H_4	One-dimensional Heis. Chain, $J = -20\,cm^{-1}$	[86]
O	Me	Me	Ph	Heis. Alt.; $J_1 = -29\,cm^{-1}$, $J_2 = -14\,cm^{-1}$	[87]
O	Me	Me	*p*-$MeOC_6H_4$	Heis. Alt.; $J_1 = -19\,cm^{-1}$, $J_2 = -9\,cm^{-1}$	[87]
O	Me	Me	*p*-MeC_6H_4	Heis. Reg., $J = -10\,cm^{-1}$	[87]
O	Me	Me	*p*-NCC_6H_4	Heis. Reg, $J = -29\,cm^{-1}$; spin-Peierls; $T_{SP} = 16$ K	[87]
O	Me	Me	*p*-$O_2NC_6H_4$	CW, $\theta = -2$ K	[87]
O	Ph	Ph	*p*-$MeOC_6H_4$	Heis. Reg; $J = -9\,cm^{-1}$	[88]
O	Ph	Ph	*p*-MeC_6H_4	CW; $\theta = +2.5$ K	[88]
O	Ph	Ph	*p*-NCC_6H_4	Heis. Reg.; $J = -9\,cm^{-1}$	[88]
O	Ph	Ph	*p*-$O_2NC_6H_4$	CW; $\theta = +1.5$ K	[88]
S	Ph	Ph	*p*-$MeOC_6H_4$	Heis. Reg.; $J = -4\,cm^{-1}$	[88]
S	Ph	Ph	*p*-MeC_6H_4	Heis. Alt.; $J_1 = -32\,cm^{-1}$, $J_2 = -22\,cm^{-1}$	[88]
S	Ph	Ph	*p*-NCC_6H_4	CW, $\theta = +2.9$ K; weak ferromagnet; $T_N = 0.41$ K	[88,89]
S	Ph	Ph	*p*-$O_2NC_6H_4$	CW, $\theta = -0.9$ K	[88,89]
O	Ph	Ph	3-Thienyl	Heis. Reg.; $J = -9\,cm^{-1}$; ferromagnetic order, $T_C = 5$ K	[90]
S	Ph	Ph	3-Thienyl	Heis. Alt.; $J_1 = -12\,cm^{-1}$, $J_2 = -7\,cm^{-1}$	[90]

[a] CW: Curie–Weiss; Heis. Reg.: regular one-dimensional Heisenberg chain; Heis. Alt: alternating chain. T_{max}: temperature at which χ reaches maximum value.

56$Me^+(TCNQ)_2^-$ although no crystal structure of this material is available. The other 1:2 salts have magnetic properties that were not amenable to modelling using simple combinations of singlet–triplet models, magnetic chains and Curie impurities. Once again, the absence of structural data is a major impediment, and the titling of this class of compounds as "genuine magnetic semiconductors" is a curious one because the compounds in question are not "magnetic" in the ordered sense.

Related to the TCNQ/verdazyl systems are metal bis(dithiolene) salts of trialkylammonium cation—substituted verdazyls **57–59** [93,94]. The physical properties of all compounds are summarized in Table 3. Crystallographic characterization was obtained for the three 1:1 salts **57**$^+$ $[Ni(dmit)_2]^-$, **58**$^+$ $[Ni(dmit)_2]^-$ and **59**$^+$ $[Ni(dmit)_2]^-$. All of these contain relatively isolated verdazyl-substituted cations and the $Ni(dmit)_2$ anion, which associates into weakly bound dimers as depicted in Fig. 10 for the salt of **57**$^+$. The

Table 2
Physical properties of TCNQ salts of *N*-alkylpyridinium verdazyls [91,92]

Compound	σ_{RT} (S cm^{-1})	E_A (eV)	Magnetism
55Me^+ $TCNQ^-$	1.3×10^{-6}	–	CW; $\theta = +2.1$ K
55Et^+ $TCNQ^-$	2×10^{-6}	–	AF interactions; no modelling
55$Me^+(TCNQ)_2^-$	8.1×10^{-3}	0.092	AF interactions; no modelling
55$Et^+(TCNQ)_2^-$	6.9×10^{-2}	0.072	Dimer model, $J = -66\,cm^{-1}$
56Me^+ $TCNQ^-$	1.1×10^{-7}	–	Heis. Alt. Chain, ($J_1 = -16\,cm^{-1}$, $J_2 = -14.7\,cm^{-1+}$), +ST ($J = -220\,cm^{-1}$)
56Et^+ $TCNQ^-$	1.3×10^{-7}	–	AF interactions; no modelling
56$Me^+(TCNQ)_2^-$	2.9×10^{-2}	0.091	AF interactions; no modelling
56$Et^+(TCNQ)_2^-$	1.1×10^{-3}	0.25	Heis. Alt. Chain, ($J_1 = -5.3\,cm^{-1}$, $J_2 = -2.1\,cm^{-1+}$), +ST ($J = -257\,cm^{-1}$)

Table 3
Properties of $M(dmit)_2$ salts of oxoverdazyl-based cations **57–59** [93,94]

Compound	σ_{RT} (S cm^{-1})	E_A (eV)	Magnetism
57$^+$ $[Ni(dmit)_2]^-$	3.6×10^{-7}	–	CW ($\theta = -5$ K) + one-dimensional Alt chain ($J_1 = -95$ cm^{-1}, $J_2 = -19$ cm^{-1})
57$^+$ $[Ni(dmit)_2]_3^-$	8.9×10^{-2}	0.11	CW ($q = -5$ K) + S–T ($J = -89.7$ cm^{-1})
57$_2^+$ $[Zn(dmit)_2]^{2-}$	3.0×10^{-4}	–	CW, $\theta = -2.8$ K
57$_2^+$ $[Pd(dmit)_2]^{2-}$	1.3×10^{-4}	0.40	CW, $\theta = -3.1$ K
57$_2^+$ $[Pt(dmit)_2]^{2-}$	1.8×10^{-7}	–	CW, $\theta = -2.6$ K
58$^+$ $[Ni(dmit)_2]^-$	1.8×10^{-7}	–	CW ($\theta = -0.4$ K) + S–T ($J = -123$ cm^{-1})
59$^+$ $[Ni(dmit)_2]$	4.7×10^{-5}	–	Linear tetramer ($J_1 = -10.4$ cm^{-1}m $J_2 = -201$ cm^{-1})

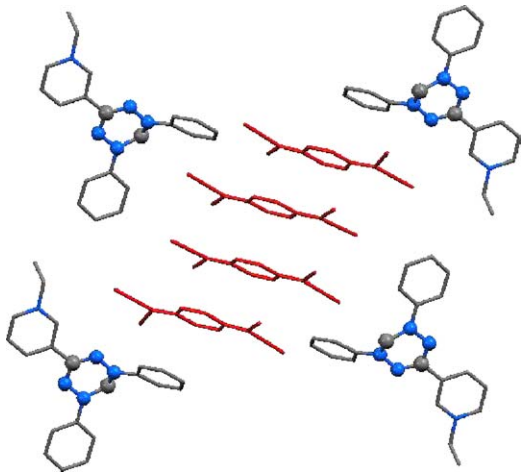

Fig. 9. Packing diagram for **56**Et$^+$$(TCNQ)_2^-$ [92].

N–S distances are 3.58 Å apart, suggesting that spin pairing may not be complete, and indeed the magnetism of the compounds containing these dimeric species contains singlet–triplet models with moderately strong exchange energies (−100 to −200 cm^{-1}). As was the case for the TCNQ salts, the "mixed valent" salts here are semiconducting while the 1:1 salts are insulators. Magnetically the systems are not unlike the TCNQ salts in that the overall properties can generally be described as the sum of a relatively strong π-dimer interaction involving radical anions with Curie–Weiss behaviour derived from the cations.

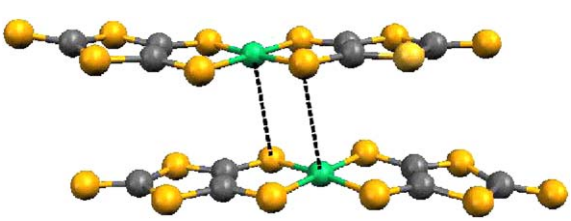

Fig. 10. Molecular structure of the dimer of the $Ni(dmit)_2$ anion in **57**$^+$ $[Ni(dmit)_2]^-$ [93].

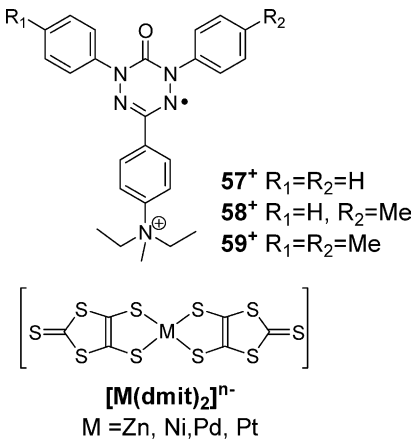

A somewhat different "salt" based approach has been explored in which the verdazyl radical itself is employed as an electron donor [95]. A series of 1,3,5-triarylverdazyls **60** (R = H, Me, OMe) were reacted with strong electron acceptors such as $TCNQF_4$ or DDQ (Scheme 5). In these cases, complete electron transfer from radical to acceptor occurred, leading to "verdazylium" salts of the acceptor radical anion. The X-ray structure of one derivative reveals that the $TCNQF_4$ radical anions form π-dimers; as such, both cationic and anionic moieties are $S = 0$ entities in the solid state and all of the derivatives of this class are accordingly essentially diamagnetic.

3.4. Metal complexes of verdazyl radicals

One of the most fruitful areas of research into "heterospin" systems are metal complexes in which spins reside both

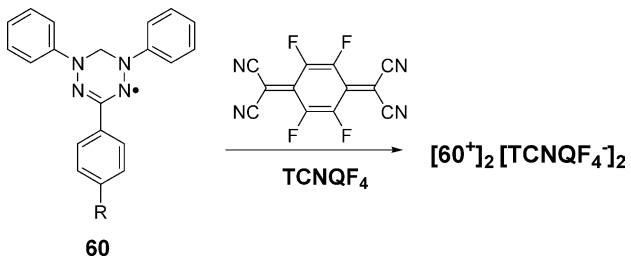

Scheme 5.

on the metal ion and one or more ligands directly coordinated to the metal. This so-called "hybrid" approach combines organic (π) and metal (d) based spins and has led to a huge number of metal–radical complexes with a wide range of physicochemical properties. The major classes of radical-based ligands are nitroxides (including nitronyl nitroxides and imino nitroxides) [96], semiquinones [97,98] and radical anions of TCNE and TCNQ and other species [99,100].

The coordination chemistry of verdazyl radicals is still in its early stages of development. The first coordination complexes of a verdazyl were reported by Brook et al.'s a series of Cu(I) complexes of the bis(verdazyl) **30** described in Section 3 [101]. Each diradical simultaneously binds to two Cu(I) ions in a bis-bidentate mode, and the copper ion coordination sphere is completed by bridging halides giving rise to one-dimensional coordination polymers represented schematically by **61–63**. The magnetic susceptibility of the three complexes is qualitatively very similar, with maxima in the χ versus T plots indicative of low-dimensional antiferromagnetic exchange. The data were modelled based on an alternating one-dimensional chain consisting of two exchange parameters J_1 and J_2, where the former was ascribed to the intramolecular spin–spin interaction within each diradical, while the latter is ascribed to interchain interactions between pairs of radicals. The exchange parameters were determined to be as follows: for **61**, $J_1 = -190\,\mathrm{cm}^{-1}$ and $J_2 = -116\,\mathrm{cm}^{-1}$; **62**, $J_1 = -200\,\mathrm{cm}^{-1}$ and $J_2 = -110\,\mathrm{cm}^{-1}$; **63**, $J_1 = -271\,\mathrm{cm}^{-1}$ and $J_2 = -200\,\mathrm{cm}^{-1}$. The significantly different parameters for the iodide-based material **63** may be due to a different packing pattern—powder X-ray diffraction studies suggest it has a different unit cell than **61** or **62** (which are isostructural), though single crystal data for **63** are lacking.

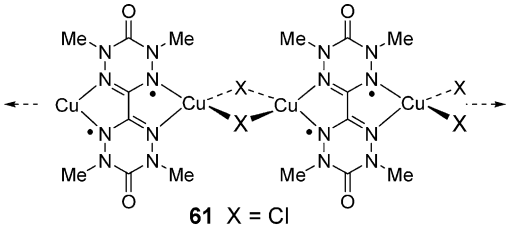

61 X = Cl
62 X = Br
63 X = I

Although intrachain exchange mediated by Cu–X–Cu bridges was thought to be negligible, the change in the intramolecular J_1 of the coordinated molecules of **30** compared to the exchange interaction in free **30** suggests strong modulation of the electronic structure of the diradical via coordination, even to a diamagnetic metal ion. This hypothesis was examined computationally in model dinuclear compounds **64** in which the exchange interaction in the diradical was examined as a function of the phosphines PR_3. Density functional calculations suggest that stronger phosphine donors lead to smaller antiferromagnetic exchange interactions [31].

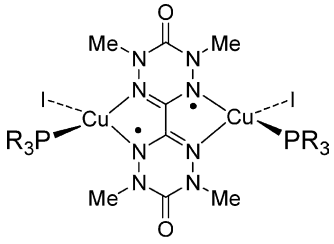

64

Discrete verdazyl-coordination complexes of diamagnetic metal ions have been realized by using a verdazyl radical **64** containing a 2-pyridyl substituent. This radical was designed to chelate to a single metal analogously to 2,2′-bipyridine [102]. Group 12 dihalide complexes **66** (MX_2 = $ZnCl_2$, CdI_2, $HgCl_2$) were made either by direct reaction of the radical with the metal dihalide or by initial coordination of the radical precursor, i.e. the corresponding tetrazane, followed by oxidation of the coordinated tetrazane to a radical [103]. Cationic copper(I) bis-phosphine complexes **67** were generated in situ from the radical, $[Cu(MeCN)_4]^+$ and the phosphine [104]. The metal–radical complexes could be characterized in solution but no structural or solid-state magnetic data could be obtained owing to the decomposition of the complexes regardless of the way in which they were prepared. Nonetheless, simulation of the EPR spectra of the metal complexes suggested some perturbation of the radical electronic structure—selected nitrogen hyperfine coupling constants increase upon coordination by up to 2G and in the Cu complexes, additional hfcs could be given to the Cu and the P atoms.

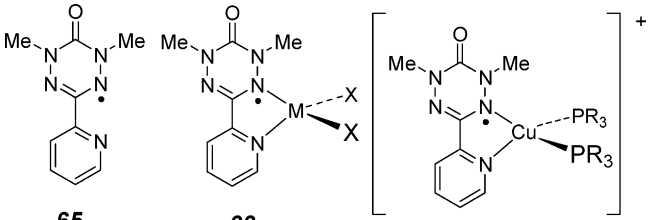

65 **66** **67**

One tetrazane complex did lead to isolation of a binuclear CuBr adduct **68** of verdazyl **65**, basically a model segment of the polymer network **62** [105]. Oxidation was affected by air in reaction, and was perhaps catalyzed by the metal ion. Magnetic measurement shows only weak antiferromagnetic interactions which could not be quantifiably modelled, although an exchange parameter of $\sim -10\,\mathrm{cm}^{-1}$ was estimated based on a dimer model; through-space intermolecular interactions between neighbouring radicals may well be the primary exchange mechanism here.

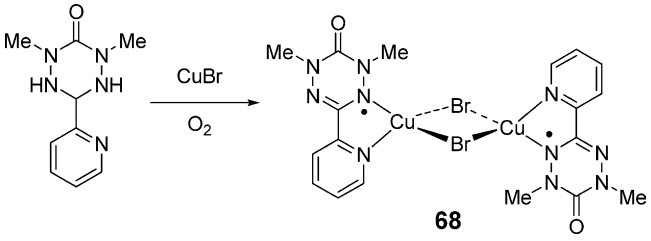

68

A few other verdazyl complexes of diamagnetic metal ions have been reported. Hicks and co-workers prepared a 2:1 homoleptic, mononuclear Cu(I) complex **69** of a 6-methyl-2-pyridyl analogue of radical **65** [106]. Structurally, the two radicals are not perpendicular to one another, as the Cu(I) coordination geometry is a flattened tetrahedron. Despite the coordination of two radicals to a single metal ion, the intramolecular radical–radical exchange in this cationic species was found to be very weak ($\sim -2\,cm^{-1}$), in contrast to a related bis(imino nitroxide)Cu(I) complex in which the two radicals are fairly strongly ferromagnetically coupled [107]. Computational studies suggest that the geometry at the copper center indeed has a strong effect on the intramolecular radical–radical exchange [108].

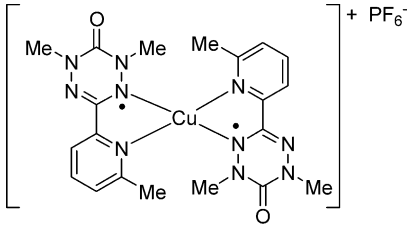

69

The only other verdazyl complex of a diamagnetic metal ion is a $Ru(Bipy)_2^{2+}$ complex **70** of an *N*-methylpyrazole substitued verdazyl. The compound was spectroscopically and electrochemically characterized but no magnetic properties were reported [109].

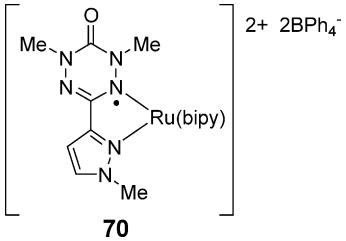

70

Radical complexes of paramagnetic metal ions open up the possibility for direct metal–ligand exchange interactions, and it is here that some of the more significant developments in verdazyl metal chemistry can be found. The first such verdazyl complexes were the $M(hfac)_2$ complexes **71** and **72** of chelating verdazyl **65** [110]. Analysis of the magnetic susceptibility of the two complexes revealed that Mn–verdazyl intramolecular exchange is moderate and antiferromagnetic ($J = -45\,cm^{-1}$), whereas the Ni–verdazyl exchange is ferromagnetic and exceptionally strong; a lower limit of $+240\,cm^{-1}$ could be determined based on the variable temperature magnetic susceptibility. The nickel–verdazyl ferromagnetic exchange can be rationalized on the basis of orthogonality of the spin-containing orbitals (all three spins in **72** are in orbitals that share physical space, but cannot engage in quantum mechanical overlap due to symmetry constraints), and the strength of the magnetic exchange is related to the relatively large spin density on the nitrogen donor atom of the verdazyl, permitting stronger interactions with the metal-based spins. This turns out to be one of the largest ferromagnetic interactions in all of the metal–radical literature and bodes well for the magnetic properties of putative nickel–verdazyl-coordination polymers in which extended lattices of Ni(II)–verdazyl spins can interact strongly.

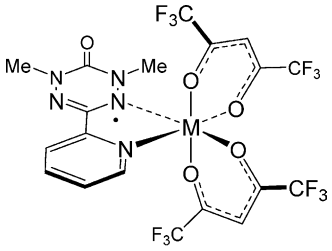

71 M = Mn
72 M = Ni

Other verdazyls (**73–75**) that have been added to the family of ligands of this radical structure have the advantage of the chelate effect to make them effective ligands. Pyrimidine-substituted verdazyl **73** is a bis-bidentate species that can coordinate to two $M(hfac)_2$ substrates analogously to the mononuclear complexes **71** and **72** [111], and the Mn– and Ni–verdazyl exchange parameters in the binuclear systems are nearly identical to those found in their mononuclear counterparts. 2:1 verdazyl:metal complexes have been prepared of verdazyls **74** [112,113] and **75** [114], and crystal structures for Ni(II) complexes of both are presented in Figs. 11 and 12, respectively. The Ni(II)–verdazyl exchange remains relatively strong and ferromagnetic and Mn(II)–verdazyl exchange is uniformly antiferromagnetic as before. However, there is some variation in the magnitude of exchange in both metal ions suggesting that magnetic interactions may be influenced by the ancillary ligand set, subtle geometry changes, etc. It is also worth noting that verdazyl–verdazyl exchange within the inner coordination sphere of a metal is highly dependent on orientation. In complexes where the radicals are not coplanar (e.g. the 2:1 complexes of **74** as well as Cu(I) complex **69**) the radical–radical interaction tends to be very weak, but in the pseudo-octahedral complexes of **75b** the two radicals lie in the same plane (cf. Fig. 12) and the radical–radical interaction becomes significant ($J = -42\,cm^{-1}$).

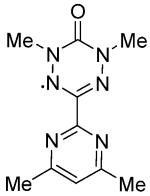

73

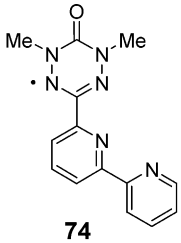

74

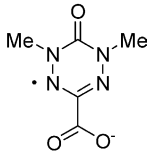

75

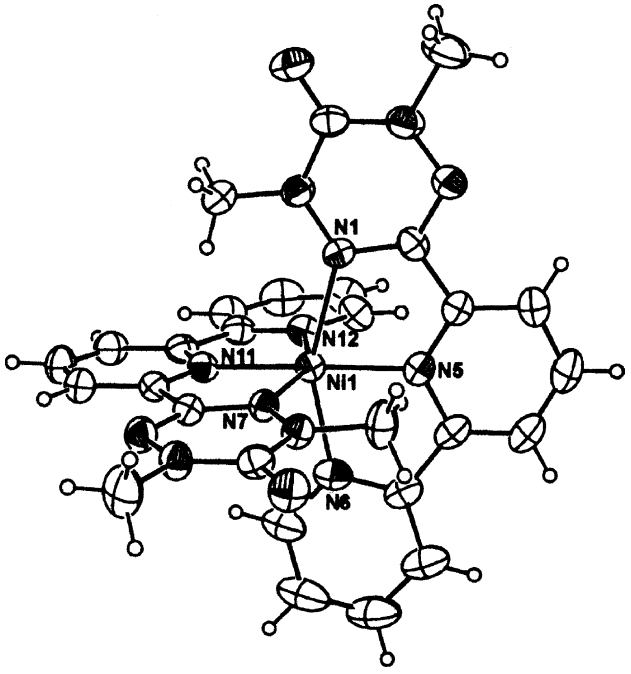

Fig. 11. ORTEP drawing of a Ni(II) complex of **74**. Reproduced from [112] with permission.

There remain some aspects of metal–verdazyl complexes that are not yet well understood. A Co(II) complex of **75** appears to exhibit ferromagnetic Co–radical exchange [114], but the quantitative modelling of exchange coupling in Co(II) centers is challenging because of the spin orbit coupling of the cobalt ion. Also, based on the orbital symmetry arguments developed for the Ni(II) systems, copper(II)–verdazyl coupling would be expected to be ferromagnetic and fairly strong similarly to nickel. Yet, the magnetism of a Cu(II) complex of **74** is very weak—all three spins are only very weakly interacting [113]. This is to date the only Cu(II) complex of a verdazyl, so more information is needed. But overall, the coordination chemistry of verdazyl radicals is proving to be a fruitful area of structural and magnetochemistry, and the structural resemblance of the verdazyl donor site to that of a pyridyl group offers much potential in the arena of metallosupramolecular chemistry. In this vein, several complex ligands **76–80** containing verdazyl ligands that are structural mimics of oligopyridines have been synthesized [115].

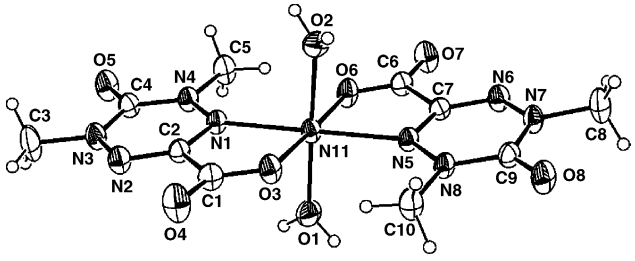

Fig. 12. ORTEP drawing of a Ni(II) complex of **75**. Reproduced from [114] with permission.

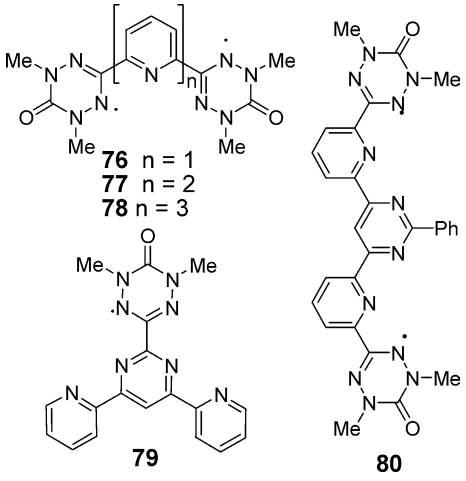

4. Conclusions

Verdazyls have a venerable history, magnetically speaking. They also deserve continued attention as magnetic building blocks: they are among the most stable of radical families, and in particular their stability towards air and water makes them well suited for use in supramolecular chemistry involving hydrogen bond donors such as OH or NH_2. A number of novel magnetic phenomena have been observed in diradicals, molecular crystals and particularly metal complexes, and the future of magnetochemistry of verdazyls should be viewed as bright.

References

[1] H. Iwamura, Pure Appl. Chem. 58 (1986) 187.
[2] A. Izuoka, S. Murata, T. Sugawara, H. Iwamura, J. Am. Chem. Soc. 109 (1987) 2631.
[3] D.A. Dougherty, Acc. Chem. Res. 24 (1991) 88.
[4] W.T. Borden, H. Iwamura, J.A. Berson, Acc. Chem. Res. 27 (1994) 109.
[5] A. Rajca, Chem. Eur. J. 8 (2002) 4834.
[6] F.A. Neugebauer, Angew. Chem. Int. Ed. Engl. 12 (1973) 455.
[7] P.F. Wiley, Chemistry of 1,2,3-Triazines and 1,2,4-Triazines, Tetrazines and Pentazines, John Wiley & Sons Inc., New York, 1978, 1225 pp.
[8] R. Kuhn, H. Trischmann, Angew. Chem., Int. Ed. Engl. 2 (1963) 155.
[9] A.W. Nineham, Chem. Rev. 55 (1955).
[10] F.A. Neugebauer, H. Fischer, Angew. Chem. Int. Ed. Engl. 19 (1980) 724.
[11] F.A. Neugebauer, H. Fischer, R. Siegel, Chem. Ber. Recl. 121 (1988) 815.
[12] F.A. Neugebauer, H. Fischer, J. Chem. Soc. Perkin Trans. 2 (1981) 896.
[13] F.A. Neugebauer, H. Fischer, C. Krieger, J. Chem. Soc. Perkin Trans. 2 (1993) 535.
[14] T.M. Barclay, R.G. Hicks, A.S. Ichimura, G.W. Patenaude, Can. J. Chem. Rev. Can. Chim. 80 (2002) 1501.
[15] R.G. Hicks, R. Hooper, Inorg. Chem. 38 (1999) 284.

[16] R.G. Hicks, L. Ohrstrom, G.W. Patenaude, Inorg. Chem. 40 (2001) 1865.
[17] P.P. Kornuta, V.N. Bobkov, O.M. Polumbrik, L.N. Markovskii, Zh. Obshch. Khim. 48 (1978) 697.
[18] A.M. Nesterenko, O.M. Polumbrik, L.N. Markovskii, J. Struct. Chem. 25 (1984) 209.
[19] D.E. Williams, Acta Crystallogr. Sect. B-Struct. Commun. B 29 (1973) 96.
[20] K. Mukai, T. Yamamoto, M. Kohno, N. Azuma, K. Ishizu, Bull. Chem. Soc. Jpn. 47 (1974) 1797.
[21] K. Mukai, H. Shikata, N. Azuma, K. Kuwata, J. Magn. Reson. 35 (1979) 133.
[22] R.L. Glazer, E.H. Poindexter, J. Chem. Phys. 55 (1971) 4548.
[23] F.A. Neugebauer, Tetrahedron 26 (1970) 4853.
[24] F.A. Neugebauer, H. Brunner, Tetrahedron 30 (1974) 2841.
[25] F.A. Neugebauer, H. Trischmann, G. Taigel, Mon. Chem. 98 (1967) 713.
[26] H. Brunner, Tetrahedron 27 (1971) 3611.
[27] F.A. Neugebauer, H. Brunner, K.H. Hausser, Tetrahedron 27 (1971) 3623.
[28] P.H.H. Fischer, Tetrahedron 23 (1967) 1939.
[29] L.N. Markovsky, O.M. Polumbrik, A.M. Nesterenko, Int. J. Quantum Chem. 16 (1979) 891.
[30] L. Ohrstrom, A. Grand, B. Pilawa, Acta Chem. Scand. 50 (1996) 458.
[31] M.T. Green, T.A. McCormick, Inorg. Chem. 38 (1999) 3061.
[32] G. Chung, D. Lee, Chem. Phys. Lett. 350 (2001) 339.
[33] I. Ciofini, C.A. Daul, Coord. Chem. Rev. 238 (2003) 187.
[34] J.M. Manriquez, G.T. Yee, R.S. McLean, A.J. Epstein, J.S. Miller, Science 252 (1991) 1415.
[35] A. Rajca, Chem. Rev. 94 (1994) 871.
[36] R. Kuhn, F.A. Neugebauer, H. Trischmann, Monatsh. Chem. 97 (1966) 525.
[37] I.M. Brown, R.W. Kreilick, J. Chem. Phys. 62 (1975) 1190.
[38] P. Kopf, K. Morokuma, R. Kreilick, J. Chem. Phys. 54 (1971) 105.
[39] F.A. Neugebauer, H. Fischer, R. Bernhardt, Chem. Ber. Recl. 109 (1976) 2389.
[40] A. Lang, H. Naarmann, G. Rosler, B. Gotschy, H. Winter, E. Dormann, Mol. Phys. 79 (1993) 1051.
[41] Y. Kurusu, H. Yoshida, M. Okawara, Tetrahedron Lett. (1967) 3595.
[42] M. Kamachi, H. Enomoto, M. Shibasaka, W. Mori, M. Kishita, Polym. J. 18 (1986) 439.
[43] W.T. Borden, E.R. Davidson, J. Am. Chem. Soc. 99 (1977) 4587.
[44] A.A. Ovchinnikov, Theor. Chim. Acta 47 (1978) 297.
[45] G. Kothe, H. Zimmerma, F.A. Neugebauer, Angew. Chem. Int. Ed. 11 (1972) 830.
[46] K. Mukai, N. Azuma, H. Shikata, K. Ishizu, Bull. Chem. Soc. Jpn. 43 (1970) 3958.
[47] N. Azuma, K. Ishizu, K. Mukai, J. Chem. Phys. 61 (1974) 2294.
[48] R.M. Fico, M.F. Hay, S. Reese, S. Hammond, E. Lambert, M.A. Fox, J. Org. Chem. 64 (1999) 9386.
[49] F.A. Neugebauer, H. Fischer, P. Meier, Chem. Ber. Recl. 113 (1980) 2049.
[50] D.J.R. Brook, H.H. Fox, V. Lynch, M.A. Fox, J. Phys. Chem. 100 (1996) 2066.
[51] V. Barone, A. Bencini, I. Ciofini, C. Daul, J. Phys. Chem. A 103 (1999) 4275.
[52] F.A. Neugebauer, Angew. Chem., Int. Ed. Engl. 6 (1967) 362.
[53] F.A. Neugebauer, R. Bernhardt, H. Fischer, Chem. Ber. Recl. 110 (1977) 2254.
[54] P.R. Serwinski, B. Esat, P.M. Lahti, Y. Liao, R. Walton, J. Lan, J. Org. Chem. 69 (2004) 5247.
[55] Y. Teki, M. Nakatsuji, Y. Miura, Int. J. Mod. Phys. B 15 (2001) 4029.
[56] Y. Teki, M. Nakatsuji, Y. Miura, Mol. Phys. 100 (2002) 1385.
[57] Y. Teki, M. Kimura, S. Narimatsu, K. Ohara, K. Mukai, Bull. Chem. Soc. Jpn. 77 (2004) 95.
[58] S. Nakatsuji, Chem. Soc. Rev. (2004) 348.
[59] M. Deumal, J. Cirujeda, J. Veciana, J.J. Novoa, Adv. Mater. 10 (1998) 1461.
[60] M. Deumal, J. Cirujeda, J. Veciana, J.J. Novoa, Chem. Eur. J. 5 (1999) 1631.
[61] N. Azuma, J. Yamauchi, K. Mukai, H. Ohyanish, Y. Deguchi, Bull. Chem. Soc. Jpn. 46 (1973) 2728.
[62] K. Takeda, H. Deguchi, T. Hoshiko, K. Konishi, K. Takahashi, J. Yamauchi, J. Phys. Soc. Jpn. 58 (1989) 3361.
[63] S. Tomiyoshi, T. Yano, N. Azuma, M. Shoga, K. Yamada, J. Yamauchi, Phys. Rev. B 49 (1994) 16031.
[64] K. Mukai, N. Azuma, K. Ishizu, Bull. Chem. Soc. Jpn. 43 (1970) 3618.
[65] N. Azuma, Bull. Chem. Soc. Jpn. 53 (1980) 2671.
[66] N. Azuma, K. Tsutsui, Y. Miura, T. Higuchi, Bull. Chem. Soc. Jpn. 54 (1981) 3274.
[67] N. Azuma, Y. Deguchi, F. Marumo, Y. Saito, Bull. Chem. Soc. Jpn. 48 (1975) 819.
[68] M. Mito, K. Takeda, K. Mukai, N. Azuma, M.R. Gleiter, C. Krieger, F.A. Neugebauer, J. Phys. Chem. B 101 (1997) 9517.
[69] P.M. Allemand, G. Srdanov, F. Wudl, J. Am. Chem. Soc. 112 (1990) 9391.
[70] H.M. McConnell, J. Chem. Phys. 39 (1963) 1910.
[71] N. Azuma, Y. Deguchi, F. Marumo, Y. Saito, Bull. Chem. Soc. Jpn. 48 (1975) 825.
[72] E. Dormann, H. Winter, W. Dyakonow, B. Gotschy, A. Lang, H. Naarmann, N. Walker, Ber. Bunsen-Ges. Phys. Chem. Chem. Phys. 96 (1992) 922.
[73] N. Azuma, Bull. Chem. Soc. Jpn. 55 (1982) 1357.
[74] K. Mukai, M. Matsubara, H. Hisatou, Y. Hosokoshi, K. Inoue, N. Azuma, J. Phys. Chem. B 106 (2002) 8632.
[75] R.G. Hicks, M.T. Lemaire, L. Ohrstrom, J.F. Richardson, L.K. Thompson, Z.Q. Xu, J. Am. Chem. Soc. 123 (2001) 7154.
[76] R.K. Kremer, B. Kanellakopulos, P. Bele, H. Brunner, F.A. Neugebauer, Chem. Phys. Lett. 230 (1994) 255.
[77] K. Mukai, M. Yanagimoto, Y. Shimobe, K. Inoue, Y. Hosokoshi, Chem. Phys. Lett. 311 (1999) 446.
[78] K. Mukai, K. Suzuki, K. Ohara, J.B. Jamali, N. Achiwa, J. Phys. Soc. Jpn. 68 (1999) 3078.
[79] K. Mukai, M. Yanagimoto, S. Narimatsu, H. Maruyama, Y. Narumi, K. Kindo, J. Phys. Soc. Jpn. 71 (2002) 2539.
[80] K. Mukai, M. Yanagimoyo, S. Tanaka, M. Mito, T. Kawae, K. Takeda, J. Phys. Soc. Jpn. 72 (2003) 2312.
[81] K. Mukai, K. Oishi, K. Ishizu, N. Azuma, Chem. Phys. Lett. 23 (1973) 522.
[82] K. Mukai, K. Nedachi, J.B. Jamali, N. Achiwa, Chem. Phys. Lett. 214 (1993) 559.
[83] K. Mukai, K. Nedachi, M. Takiguchi, T. Kobayashi, K. Amaya, Chem. Phys. Lett. 238 (1995) 61.
[84] K. Mukai, K. Konishi, K. Nedachi, K. Takeda, J. Magn. Magn. Mater. 140 (1995) 1449.
[85] K. Mukai, K. Konishi, K. Nedachi, K. Takeda, J. Phys. Chem. 100 (1996) 9658.
[86] K. Mukai, S. Kawasaki, J.B. Jamali, N. Achiwa, Chem. Phys. Lett. 241 (1995) 618.
[87] K. Mukai, N. Wada, J.B. Jamali, N. Achiwa, Y. Narumi, K. Kindo, T. Kobayashi, K. Amaya, Chem. Phys. Lett. 257 (1996) 538.
[88] K. Mukai, M. Nuwa, K. Suzuki, S. Nagaoka, N. Achiwa, J.B. Jamali, J. Phys. Chem. B 102 (1998) 782.
[89] K. Mukai, M. Nuwa, T. Morishita, T. Muramatsu, T.C. Kobayashi, K. Amaya, Chem. Phys. Lett. 272 (1997) 501.
[90] K. Balluder, M. Kelemen, F. Perez, B. Pilawa, C. Wachter, E. Dormann, Ber. Bunsen-Ges. Phys. Chem. Chem. Phys. 101 (1997) 1882.

[91] K. Mukai, S. Jinno, Y. Shimobe, N. Azuma, Y. Hosokoshi, K. Inoue, M. Taniguchi, Y. Misaki, K. Tanaka, Polyhedron 20 (2001) 1537.
[92] K. Mukai, S. Jinno, Y. Shimobe, N. Azuma, M. Taniguchi, Y. Misaki, K. Tanaka, K. Inoue, Y. Hosokoshi, J. Mater. Chem. 13 (2003) 1614.
[93] K. Mukai, T. Hatanaka, N. Senba, T. Nakayashiki, Y. Misaki, K. Tanaka, K. Ueda, T. Sugimoto, N. Azuma, Inorg. Chem. 41 (2002) 5066.
[94] K. Mukai, N. Senba, T. Hatanaka, H. Minakuchi, K. Ohara, M. Taniguchi, Y. Misaki, Y. Hosokoshi, K. Inoue, N. Azuma, Inorg. Chem. 43 (2004) 566.
[95] S. Nakatsuji, A. Kitamura, A. Takai, K. Nishikawa, Y. Morimoto, N. Yasuoka, H. Kawamura, H. Anzai, Z. Naturforsch. B 53 (1998) 495.
[96] (a) A. Caneschi, D. Gatteschi, P. Rey, Prog. Inorg. Chem. 39 (1991) 331;
(b) H. Iwamura, K. Inoue, in: J.S. Miller, M. Drillon (Eds.), Magnetism: Molecules to Materials II, Wiley/VCH, Weinheim, 2001, p. 60.
[97] C.G. Pierpont, R.M. Buchanan, Coord. Chem. Rev. 38 (1981) 45.
[98] (a) C.G. Pierpont, C.G. Lange, Prog. Inorg. Chem. 41 (1994) 331; (b) D.A. Shultz, in: J.S. Miller, M. Drillon (Eds.), Magnetism: Molecules to Materials II, Wiley/VCH, Weinheim, 2001, p. 281.
[99] W. Kaim, Coord. Chem. Rev. 76 (1987) 187.
[100] W. Kaim, M. Moscherosch, Coord. Chem. Rev. 129 (1994) 157.
[101] D.J.R. Brook, V. Lynch, B. Conklin, M.A. Fox, J. Am. Chem. Soc. 119 (1997) 5155.
[102] C.L. Barr, P.A. Chase, R.G. Hicks, M.T. Lemaire, C.L. Stevens, J. Org. Chem. 64 (1999) 8893.
[103] D.J.R. Brook, S. Fornell, J.E. Stevens, B. Noll, T.H. Koch, W. Eisfeld, Inorg. Chem. 39 (2000) 562.
[104] D.J.R. Brook, V. Abeyta, J. Chem. Soc. Dalton Trans. (2002) 4219.
[105] D.J.R. Brook, S. Fornell, B. Noll, G.T. Yee, T.H. Koch, J. Chem. Soc. Dalton Trans. (2000) 2019.
[106] T.M. Barclay, R.G. Hicks, M.T. Lemaire, L.K. Thompson, Inorg. Chem. 40 (2001) 6521.
[107] H. Oshio, T. Watanabe, A. Ohto, T. Ito, T. Ikoma, S. TeroKubota, Inorg. Chem. 36 (1997) 3014.
[108] J.E. Stevens, D.J.R. Brook, V.W. Abeyta, Polyhedron 22 (2003) 2241.
[109] J.Z. Wu, E. Bouwman, J. Reedijk, A.M. Mills, A.L. Spek, Inorg. Chim. Acta 351 (2003) 326.
[110] R.G. Hicks, M.T. Lemaire, L.K. Thompson, T.M. Barclay, J. Am. Chem. Soc. 122 (2000) 8077.
[111] T.M. Barclay, R.G. Hicks, M.T. Lemaire, L.K. Thompson, Inorg. Chem. 40 (2001) 5581.
[112] T.M. Barclay, R.G. Hicks, M.T. Lemaire, L.K. Thompson, Chem. Commun. (2000) 2141.
[113] T.M. Barclay, R.G. Hicks, M.T. Lemaire, L.K. Thompson, Inorg. Chem. 42 (2003) 2261.
[114] T.M. Barclay, R.G. Hicks, M.T. Lemaire, L.K. Thompson, Z.Q. Xu, Chem. Commun. (2002) 1688.
[115] R.G. Hicks, B.D. Koivisto, M.T. Lemaire, Org. Lett. 6 (2004) 1887.
[116] A.R. Katritzky, S.A. Belyakov, Synthesis (1997) 17.